

Non-stationary statistical modeling of extreme wind speed series with exposure correction

Mingfeng Huang¹, Qiang Li¹, Haiwei Xu^{*1}, Wenjuan Lou¹ and Ning Lin²

¹Institute of Structural Engineering, College of Civil Engineering & Architecture, Zhejiang University, Hangzhou 310058, China

²Department of Civil and Environmental Engineering, Princeton University, Princeton, New Jersey, USA

(Received October 18, 2017, Revised January 10, 2018, Accepted January 13, 2018)

Abstract. Extreme wind speed analysis has been carried out conventionally by assuming the extreme series data is stationary. However, time-varying trends of the extreme wind speed series could be detected at many surface meteorological stations in China. Two main reasons, exposure change and climate change, were provided to explain the temporal trends of daily maximum wind speed and annual maximum wind speed series data, recorded at Hangzhou (China) meteorological station. After making a correction on wind speed series for time varying exposure, it is necessary to perform non-stationary statistical modeling on the corrected extreme wind speed data series in addition to the classical extreme value analysis. The generalized extreme value (GEV) distribution with time-dependent location and scale parameters was selected as a non-stationary model to describe the corrected extreme wind speed series. The obtained non-stationary extreme value models were then used to estimate the non-stationary extreme wind speed quantiles with various mean recurrence intervals (MRIs) considering changing climate, and compared to the corresponding stationary ones with various MRIs for the Hangzhou area in China. The results indicate that the non-stationary property or dependence of extreme wind speed data should be carefully evaluated and reflected in the determination of design wind speeds.

Keywords: extreme wind speed; exposure adjustment; non-stationary; statistical modeling; generalized maximum likelihood approach

1. Introduction

Wind loads impacting on engineering structures are largely dependent on the strength of wind speeds, which could be represented by the extreme wind speed quantiles (design wind speeds) associated with various mean recurrence intervals (MRIs) for a particular site. According to the Chinese load code (GB 50009-2012), the design wind speeds can be estimated from the statistical modeling of annual maximum 10-min mean wind speed data obtained from meteorological stations in China. Based on the existing studies, it is widely acceptable to utilize one of the distributions from the generalized extreme value (GEV) family to model the extreme wind speeds when the recorded wind speed data is enough and adequate to allow fitting of the distribution function with a reasonable error margin (Tuller and Brett 1984, Pavia and O'Brien 1986). Many studies (Cook 1985, Simiu and Heckert 1996, Palutikof *et al.* 1999, Cook and Harris 2004, Kasperski 2009, Harris 2009) suggested that the Gumbel distribution, the simplest case of the GEV family, is the effective model to represent the distribution of extreme wind speeds. Similar to many wind load codes, the Chinese load code also adopts the Gumbel model to analyze the annual maximum wind speed series. In addition to the extreme wind speed distribution, researchers found that the parent wind speed population

could be properly described by the Weibull model or hybrid Weibull model (Kasperski 2009). Recently Harris and Cook (2014) proposed a new distribution that supports the Weibull distribution as the cumulative distribution function (CDF) for parent wind speeds. Pagnini and Solari (2015) proposed a joint modeling of the parent population and extreme value distribution of wind speed based on hybrid Weibull model and obtained an analytical expression of the modification coefficients for design wind speed with various MRIs that can be applied in engineering practice.

In the classical extreme value analysis, extreme wind speed data collected from a study area should be assumed to be independently and identically distributed in a stationary extreme wind speed climate (Coles 2001). However, several literatures in the meteorological and geophysical fields have revealed that the statistics of extreme climate variables (e.g., extreme temperature, extreme precipitation and extreme wind speed) were changing with time over the last decades and might continue to change in the near future under the background of global warming attributable to human activity (Zwiers and Kharin 1998, Yan *et al.* 2006, Hindecha *et al.* 2008, Lombardo and Ayyub 2015, Ruest *et al.* 2016). In recent studies, Lombardo and Ayyub (2015) analyzed the extreme wind and heat events in Washington, DC, area and observed a slight overall decrease in annual maximum gust wind speeds over the last 50-70 years. The decreasing trend in observed gust wind speeds were attributed to non-climate, climate and human factors (Lombardo 2012, 2014). Mo *et al.* (2015) carried out the regression and t-test analyses to the annual maximum 10-min mean wind speed series from 194 meteorological

*Corresponding author, Lecturer'
E-mail: haiwei163@163.com

stations in China and revealed the existence of temporal trends in surface wind speed observations from 166 stations. The annual mean wind speeds over broad areas of China were also found temporally decreasing (Xu *et al.* 2006, Jiang *et al.* 2010, You *et al.* 2011, Li *et al.* 2012, Yang *et al.* 2012). Therefore, it is necessary to investigate the non-stationarity of extreme wind speeds in China considering a changing climate. It is worth noting that many researchers from wind engineering paid attentions to the non-stationary characteristics of extreme winds, i.e., thunderstorm or downbursts and tornadoes, and their effects on structures (Xu *et al.* 2014, Huang *et al.* 2015, Aboshosha *et al.* 2015, Aboshosha and Damatty 2015). This paper is focus on the long-term non-stationarity of extreme wind speed records, which might be induced by the variation of synoptic winds, typhoons or downbursts due to the changing climate. To account for the non-stationarity in the wind speed data series, the covariate method is normally used to model the temporal trends in the parameters of the extreme value distribution (Coles 2001, Katz *et al.* 2002, Kharin and Zwiers 2005, Hinde *et al.* 2008). The so-called covariate method is implemented by modeling one or more of the distribution parameters as linear or nonlinear functions of the covariates such as time on which the recorded data series show certain level of dependence. Zhang *et al.* (2004) pointed out that the covariate method is quite effective for detect the possible non-stationary trends in extreme climate data series.

The Chinese load code specifies that the 10-min mean wind speed should be observed at the reference height of 10 m for open rural exposure in the meteorological stations. However, attributable to the rapid urbanization in China since 1980s, the terrain near the meteorological station might have changed dramatically so that the exposure category in the vicinity of the original anemometer site might become very different from the initial open rural exposure. Therefore it is questionable to directly utilize the original wind speed series for statistical modeling to estimate the basic design wind speed without any terrain correction. As specified in AIJ-RLB (2004), the wind speed series of different years were classified into different exposure categories according to the observed gust factors measured by meteorological stations in Japan. Sacré *et al.* (2007) utilized the geographical information system to classify the terrain roughness in France. Chen *et al.* (2012) tried to correct the annual maximum wind speed data from two meteorological stations in China based on the empirical relationship between the gust factor and the roughness length proposed by Ashcroft (1994). Mo *et al.* (2015) applied this exposure correction procedure by considering the directional dependent adjustment for exposure and used the reanalysis data to explore the spatial and temporal trends of the extreme wind speed for 151 meteorological stations in China. It should be noted that the exposure correction procedure proposed by Chen *et al.* (2012) needs the information of gust factors based on the observed daily maximum 10-min mean wind speed together with the 3-s gust wind speed. However, the 3-s gust wind speed is not a statutory observed item for each meteorological station in China so that the corresponding gust factors might not be

always available.

There are two main objectives in this study. One is aimed at investigating the existence of any temporal trend in the original wind speed data affected by the time varying exposure for the Hangzhou area in China and then attempting to correct these data series to obtain the adjusted wind speed data corresponding to the standard condition referenced in the Chinese load code (i.e., the 10-min mean wind speed at 10 m height for open rural exposure). The exposure correction in this study was applied into both the daily maximum and the annual maximum wind speed series. The second objective is to evaluate the non-stationarity of the extreme wind speed data series considering a long-term changing climate. A non-stationary statistical modeling method that incorporates time as a covariate was used to model the distribution parameters of the extreme wind speeds in the presence of a long-term temporal trend. The generalized maximum likelihood (GML) approach was adopted to estimate the distribution parameters. Based on the adjusted daily/annual maximum wind speed data, the non-stationary extreme wind speed quantiles were estimated and compared to the corresponding stationary ones with various MRIs.

2. Correction of wind speed data for time varying exposure

2.1 Study area and wind speed data specification

The wind speed data series of the Hangzhou (China) meteorological station are publically available in the China Meteorological Data System (CMDS) (<http://data.cma.cn/>). Since the Hangzhou meteorological station belongs to the international exchange ground meteorological stations (IEGMS), standard practice for data quality control is warranted. According to the meteorological data specification, the collected wind speed data has been carefully calibrated by adjusting the observation height, observation time interval and so on to the standard condition. Wind speed data measured at 10 m height in the Hangzhou meteorological station over the period from 1968 to 2013 were utilized to estimate the extreme wind speeds in Hangzhou area with various MRIs. The recorded data series include daily maximum 10-min mean wind speed at 10 m height, along with its corresponding wind direction sector and the 3-s gust mean wind speed. Fig. 1 shows the characteristics of the existing surrounding terrain of Hangzhou meteorological station site, in which the radius of white circle is 1 km. The topographical change nearby Hangzhou meteorological station is also shown in Figs. 2(a) and 2(b). Two photos were shot at the same location at the Hangzhou meteorological station and the buildings in the photos were both located in the east of the Hangzhou station. As shown in Figs. 2(a) and 2(b), most of low-rise buildings built before 1980s were removed and replaced by modern high-rise buildings. Therefore, a qualitative conclusion can be made that the existing exposure category for the Hangzhou meteorological station is far from the open rural exposure attributable to the rapid urban

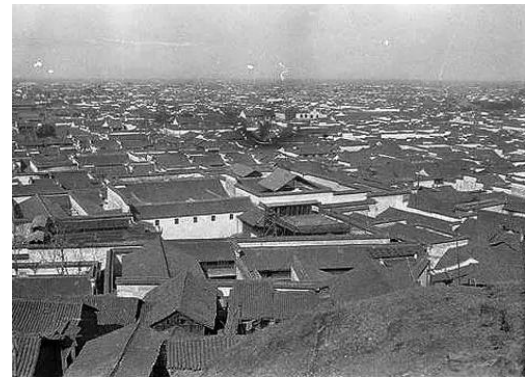
development and construction.

Daily maximum 10-min mean wind speeds were recorded during the years of 1968 to 2013 in Hangzhou meteorological station. On the other hand, the daily maximum 3-s gust wind speeds are not fully available during 1968 to 2013 with the absence in the year of 1969 and over the period from 1988 to 2001. Given the daily maximum 10-min mean wind speed series obtained from Hangzhou meteorological station, the annual maximum wind speed can also be extracted. The incident wind direction sectors for the Hangzhou meteorological station are defined in Fig. 3, where the notations D1, D2,..., D16 represent the total 16 archived wind direction sectors defined in the meteorological data specification and the 4 Roman numerals are the classified major direction sectors in order to increase the wind speed data sample size in each considered azimuth range for analyzing the gust factors and roughness lengths, which would be used for exposure correction.

Since the Hangzhou area has a mixed wind climate, it receives its extreme wind speed from different storm types including tropical cyclones (TCs) and extra-tropical cyclones such as monsoons. Note that it is expected that thunderstorm downburst may occur in coastal Hangzhou because this type of winds have been reported in other coastal areas (e.g., Solari *et al.* 2012). In this paper, an effort was made to identify the TC-induced extreme wind speed data from the derived wind speed series of Hangzhou station using the CMA-STI Best Track Dataset for Tropical Cyclones over the western North Pacific compiled by China Meteorological Administration (CMA) and Shanghai Typhoon Institute (STI). The detailed specification of CMA-STI Best Track Dataset can be referred to the work of Ying *et al.* (2014) and the dataset can be obtained from the website (www.typhoon.gov.cn). It is assumed that the surface wind speed series of Hangzhou station are dominated by a TC when the shortest distance from the anemometer site to the TC's center is less than 600 km. Table 1 lists the meteorological statistics of annual maximum wind speeds of Hangzhou station from 1968 to 2013. From Table 1, it can be found that there are 11 TCs in the history affecting the annual maximum wind speed series of Hangzhou station.



Fig. 1 Existing surrounding terrain of Hangzhou meteorological station (from Google Earth, circle radius is 1 km)



(a) Photoed before 1980s



(b) Photoed in 2016

Fig. 2 Topographical change in the east of Hangzhou meteorological station

The maximum value (i.e., 23.0 m/s) of the wind speed series over the 46 years is observed on 8 August 1988, when typhoon Bill passed by Hangzhou within a 25 km distance. By excluding the 11 extreme wind speed series affected by TCs, the rest 35 annual maximum wind speed series are found mostly occurred from November to April, the corresponding main wind directions are observed mostly from northwest to northeast. Therefore, it can be demonstrated that the extreme wind speeds of Hangzhou area are indeed related to the mixed wind climate, which mainly consists of typhoons and the east Asian winter monsoons. Since each storm type is characterized by its own probability distribution, the extreme wind speeds for mixed wind climate regions could be described by a mixed distribution based on the individual distributions of those storm types (Lombardo *et al.* 2009). However, the observed typhoon wind speed in Hangzhou region is very limited with only 11 data (less than 1/4) of the total 46 annual maximum wind speeds. It is difficult to derive the individual probability distribution from the very limited number of the extreme typhoon wind speeds for Hangzhou, which is not a typhoon-prone area. Furthermore, the design wind speed specified in the Chinese load code (GB 50009-2012) is derived from the annual maximum wind speed data without separation for storm types. In order to make a fair comparison to the code values, the typhoon wind speed records from the Hangzhou station are still included in the analysis of the data in this paper.

Table 1 Meteorological statistics of annual maximum wind speeds of Hangzhou station

Year	Annual max. wind speed (m/s)	Wind direction	Occurrence date	TC's No.	TC's name	Intensity category	Shortest distance
1968	14.2	16	8-Nov				
1969	16.0	16	4-Apr				
1970	14.0	15	17-Apr				
1971	18.0	16	2-Aug				
1972	17.0	4	17-Aug	7209	BETTY	Typhoon	<300 km
1973	13.0	1	11-Apr				
1974	15.3	1	19-Aug	7413	MARY	Typhoon	<300 km
1975	14.0	1	31-Mar				
1976	16.0	15	22-Apr				
1977	13.3	16	27-Apr				
1978	15.0	16	28-Feb				
1979	13.0	16	24-Aug	7910	JUDY	Severe Tropical Storm	<300 km
1980	12.7	11	20-Jul				
1981	16.7	2	11-May				
1982	11.3	1	5-Dec				
1983	17.0	16	29-Apr				
1984	11.7	2	21-Mar				
1985	13.3	14	25-Jul				
1986	12.3	2	22-Jul				
1987	13.0	16	28-Nov				
1988	23.0	16	8-Aug	8807	BILL	Typhoon	<25 km
1989	13.0	4	16-Sep	8923	VERA	Severe Tropical Storm	<500 km
1990	16.0	16	31-Aug	9015	ABE	Typhoon	<300 km
1991	10.3	12	26-Mar				
1992	14.0	2	23-Sep	9219	TED	Severe Tropical Storm	<600 km
1993	12.0	1	7-Feb				
1994	13.0	2	25-Mar				
1995	13.3	16	22-Aug				
1996	13.0	13	27-Aug				
1997	16.3	2	19-Aug	9711	WINNIE	Typhoon	<150 km
1998	11.3	1	19-Mar				
1999	10.7	1	2-Oct				
2000	13.3	2	10-Apr				
2001	10.0	2	15-Mar				
2002	10.9	1	22-Mar				
2003	8.3	10	1-Aug				
2004	11.0	2	13-Aug	0414	RANANIM	Severe Typhoon	<250 km
2005	12.5	2	12-Sep	0515	KHANUN	Severe Typhoon	<150 km
2006	9.5	1	12-Mar				
2007	10.6	11	22-Jul				
2008	8.2	1	21-Dec				
2009	9.4	1	23-Jan				
2010	10.4	9	22-Jul				
2011	9.9	13	13-Aug				
2012	12.2	1	8-Aug	1211	HAIKUI	Severe Typhoon	<100 km
2013	11.2	1	13-Sep				

2.2 Time-varying trend test for original wind speed series

Before adjusting the original wind speed series for time varying exposure, a detection for the existence of a temporal trend in the recorded data should be implemented. The time series of the original daily maximum 10-min wind speed series at the 4 representative wind direction sectors (i.e., D1, D4, D10 and D16 defined in Fig. 3) that most frequently happen are shown in blue circles in Fig. 4. The

abscissa value in Fig. 4 refers to the sample number of the wind speed series for each direction sector and the number of the daily maximum wind speed samples in these 4 direction sectors are 2477, 1938, 2148, 1844, respectively.

A simple linear regression analysis was carried out by calculating the slopes of the estimated linear regression lines. The regression lines for the original daily maximum 10-min wind speeds in the 4 wind direction sectors are respectively depicted in Fig. 4 in blue bold lines, which clearly indicate a downward trend of daily maximum 10-

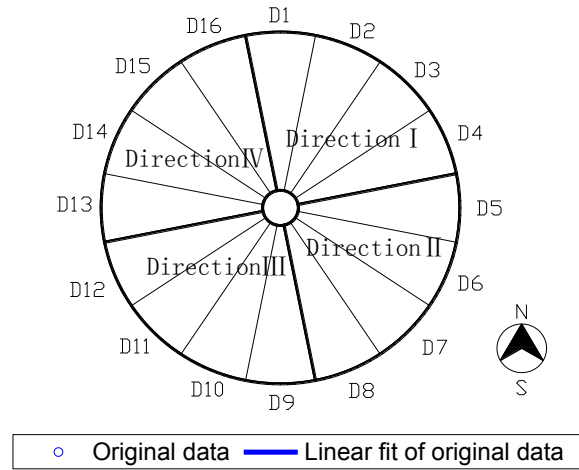


Fig. 3 Incident wind direction sectors for Hangzhou meteorological station

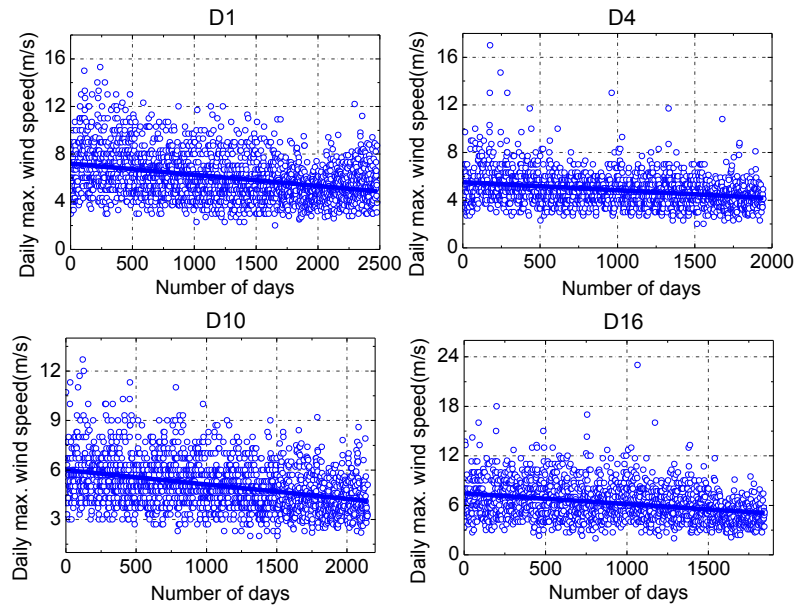


Fig. 4 Original daily maximum wind speed series and fitted linear trends for 4 representative wind direction sectors

min wind speeds over time.

A non-parametric monotonic trend test, called the Mann-Kendall (MK) test (Mann 1945, Kendall 1975, Gilbert 1987), was used to statistically assess if there is a monotonic upward or downward trend of the original daily maximum wind speed series over time. The MK test detects whether to reject the null hypothesis and accept the alternative hypothesis, where the null hypothesis is that no significant trend is detected and the alternative hypothesis is that an upward or downward trend is detected. A monotonic upward (downward) trend means that the daily maximum wind speed consistently increases (decreases) through time, but the trend may or may not be linear. The MK test can be used in place of a parametric linear regression analysis. The regression analysis requires an assumption that the residual from the estimated regression line is normally distributed, which is not required by the MK test. The MK tests on the

original daily maximum wind speed series were performed over the period from the year of 1968 to 2013. The MK test results of the daily maximum wind speed series for the 4 representative wind direction sectors are shown in Table 2. When the probability supporting the null hypothesis for the original wind speed series along one particular direction is smaller than 5%, the null hypothesis of no monotonic trend should be rejected. The computed MK test statistic Z_{MK} for the original wind speed series in the 4 representative wind direction sectors are all smaller than $-Z_{1-0.05} = -1.96$ ($Z_{1-0.05}$ is the 95% percentile of the standard normal distribution), indicating the original daily maximum wind speed series tend to decrease with time.

The original annual maximum wind speed series regardless of wind directions are shown in Fig. 5. The regression line of the original annual maximum series data is also depicted in Fig. 5 with blue solid line, in which a

Table 2 Mann-Kendall test results for the daily maximum mean wind speeds in 4 representative wind direction sectors

Wind direction		Test results	Z_{MK}	Probability of no trend
1	Before correction	Downward trend detected	-16.58	<0.01%
	After correction	Downward trend detected	-11.08	<0.01%
4	Before correction	Downward trend detected	-12.05	<0.01%
	After correction	Downward trend detected	-3.51	0.05%
10	Before correction	Downward trend detected	-17.19	<0.01%
	After correction	Downward trend detected	-11.57	<0.01%
16	Before correction	Downward trend detected	-13.70	<0.01%
	After correction	No significant trend detected	1.60	10.9%

Table 3 Mann-Kendall test results for the annual maximum mean wind speeds regardless of wind directions

	Test results	Z_{MK}	Probability of no trend
Before correction	Downward trend detected	-5.01	<0.01%
After correction	Downward trend detected	-2.81	0.49%

clear downward trend on the original annual maximum wind speed for Hangzhou station can be observed. As reported in Table 3, the MK test results of annual maximum wind speeds also confirmed the observed temporal trend with a probability supporting the null hypothesis much smaller than 0.01%.

2.3 Exposure correction

As shown in Fig. 1, the existing terrain of the Hangzhou station is quite far from the standard exposure category (i.e., Category B specified in GB 50009-2012). It is necessary to implement the exposure correction for the original wind speed records. The correction procedure can be established based on the dependency of the gust factor on the roughness length, which has been widely studied in the literature for winter storms (e.g., Ashcroft 1994) and tropical cyclones (e.g., Masters *et al.* 2010a,b, Miller *et al.* 2015). In the work of Ashcroft (1994), the observed wind speed data series were obtained from 14 British meteorological stations. The surrounding terrain of the selected stations covered a variety of terrain categories, and the obtained wind speed series were mainly affected by the cold front weather processes, which is one of the main weather processes in China. Therefore, it is practical to utilize the simplified empirical relationship between the gust factor and the roughness length advocated by Ashcroft (1994) to correct the original wind speed series of the Hangzhou station.

Given the daily maximum 10-min mean wind speed series V_{10min} and 3-s gust wind speed series V_{3sec} of Hangzhou meteorological station obtained from the CMDS, the daily 3-s gust factor $G_{3sec,d}$ can be calculated as

$$G_{3sec,d} = V_{3sec} / V_{10min} \quad (1)$$

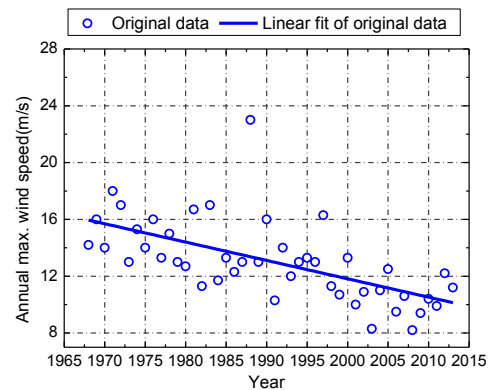


Fig. 5 Original annual maximum wind speed series and fitted linear trend for Hangzhou station

The calculated daily 3-s gust factors were grouped into 4 major wind direction sectors shown in Fig. 3 in Roman numerals in order to increase the sample size in each considered direction for estimating the median value of the time series of the gust factors for each year (denoted as G_{3sec}). It should be noted that the wind speed series that the value of V_{10min} smaller than the lower limit of 5 m/s were neglected in calculating the gust factors (Ashcroft 1994). Fig. 6 shows the fitting curves of gust factors at Direction I for two different years of 1978 and 2010, from which it can be seen that the estimated median value of the gust factor in 2010 is larger than that in 1978.

The estimated 3-s gust factors for each year can be related to the roughness length. It is usually assumed that the turbulence intensity (denoted as I_z) at the height z above the ground is a logarithmic function of the surface roughness length (denoted as z_0), the simplified form of which can be expressed as (Cook 1985)

$$I_z = A_1 + \frac{A_2}{\ln(z/z_0)} \quad (2)$$

in which the notations A_1 and A_2 are the empirical parameters determined from field observations, the recommended value of which is given in British standard (BS EN 1991-1-4: 2005) as $A_1=0, A_2=1$.

Similar to the turbulence intensity, the 3-s gust factor is also an element reflecting the characteristic of the fluctuating wind speed, the empirical relationship between I_z and G_{3sec} can be expressed as (Ashcroft 1994)

$$G_{3sec} = 1 + \gamma I_z = \hat{A}_1 + \frac{\hat{A}_2}{\ln(z/z_0)} \quad (3)$$

where the notations γ , \hat{A}_1 and \hat{A}_2 are the empirical parameters and the approximated value of \hat{A}_1 and \hat{A}_2 have been given in Ashcroft (1994) with $\hat{A}_1=1.08$, $\hat{A}_2=2.32$. It is well known the computed values of z_0 vary significantly (Masters *et al.* 2010a, b, Miller *et al.* 2015, Lombardo and Krupar 2016) even in the same wind direction sector which could significantly affect corrections. For simplicity, z_0 could be estimated by Eq. (3).

Given the empirical relationship in Eq. (3), the time-varying roughness length z_0 of the 4 major wind direction sectors can be estimated year by year. The relationship between roughness length and wind profile exponent defined in GB 50009-2012 was given in Chen *et al.* (2012) and presented in Table 4. The roughness length corresponding to the standard terrain (Category B) in GB 50009-2012 is equal to 0.05 m associated with the mean wind profile exponent of 0.16. Fig. 7 shows the estimated time varying roughness length for Hangzhou meteorological station. Since no gust wind speeds are reported over the years from 1988 to 2001, exposure correction was simply made for that period by assuming the homogeneous behavior of the change of the terrain.

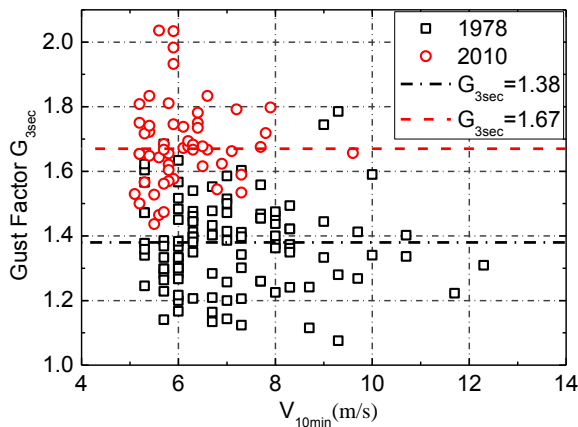


Fig. 6 Fitted curves of gust factors in Direction I for the year of 1978 and 2010

From Fig. 7, it can be observed that before 1980 the values of roughness length for the 4 major wind direction sectors are smaller than or close to 0.05 m while after 1980, attributable to the rapid urban development, the roughness lengths corresponding to 4 major wind direction sectors become greater than 0.05 m. For example, along Direction IV the roughness length over the period from 2002 to 2010 is larger than 0.3 m corresponding to Category C in GB 50009-2012 as shown in Table 4. Such time-dependent variations of roughness lengths indicate that it is necessary to adjust the original wind speed series to the standard exposure category.

The next step is to correct the mean wind speed series based on the estimated roughness length z_0 to the standard roughness length of 0.05 m. With the available daily maximum 10-min mean wind speed series V_{10min} for the time-varying exposure, the mean wind speed at the reference height of 10 m for the open rural exposure (denoted as V_0) can then be estimated as (Dyrbye and Hansen 1996)

$$V_0 = \frac{V_{10min}}{k_T \ln(10/z_0)} \quad (4)$$

where k_T is the terrain factor and can be calculated by

$$k_T = 0.19(z_0/0.05)^{0.07} \quad (\text{BS EN 1991-1-4: 2005}).$$

By using Eq. (4), the corrected daily maximum wind speed series and the annual maximum wind speed series can be obtained. Since the roughness length values are slightly smaller than or close to 0.05 m before 1980 as shown in Fig.7, it is reasonable to speculate that the terrain around Hangzhou meteorological station was kept the same as the standard exposure of Category B in GB 20009-2012 during that period. That is to say, only the estimated roughness lengths for the 4 major wind direction sectors after 1980 were utilized to correct the original wind speed series in this paper.

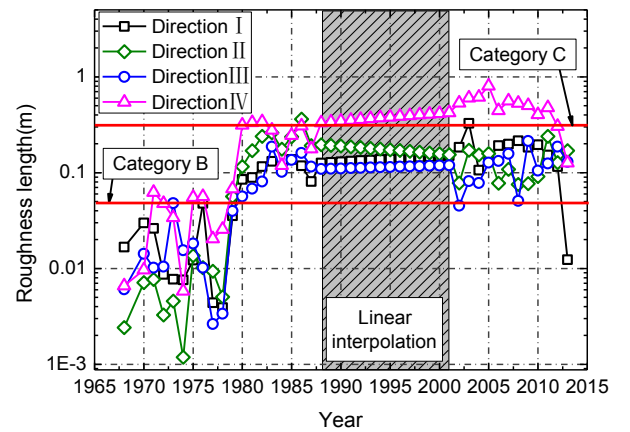


Fig. 7 Time varying roughness length and fitted curves of Hangzhou meteorological station

Table 4 Relationship between roughness length and mean wind speed profile exponent defined in GB 50009-2012

Exposure category	Description	Roughness length	Mean profile exponent
A	Open sea	0.01	0.12
B (Standard)	Rural area	0.05	0.16
C	Urban area	0.30	0.22
D	City center	1.00	0.30

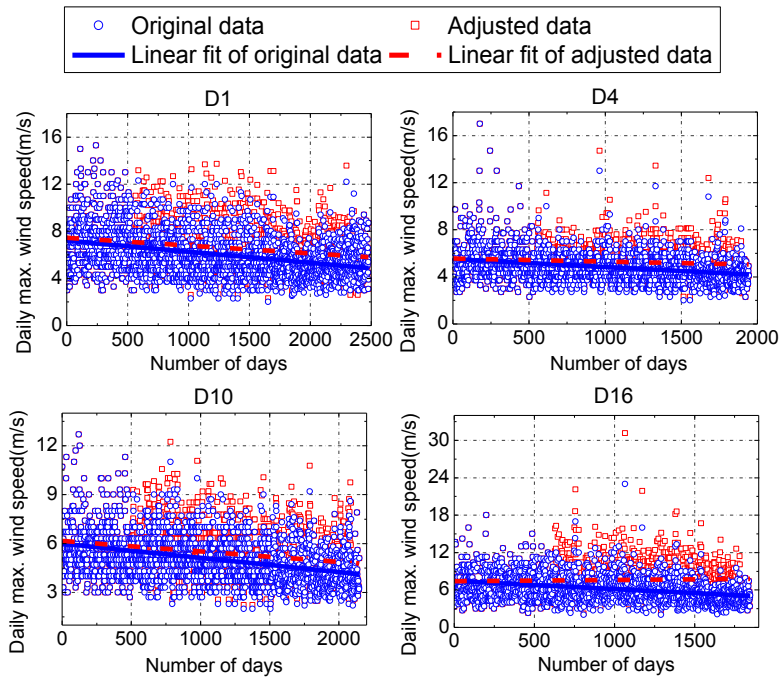


Fig. 8 Comparison between adjusted and original daily maximum wind speed series for 4 representative wind direction sectors

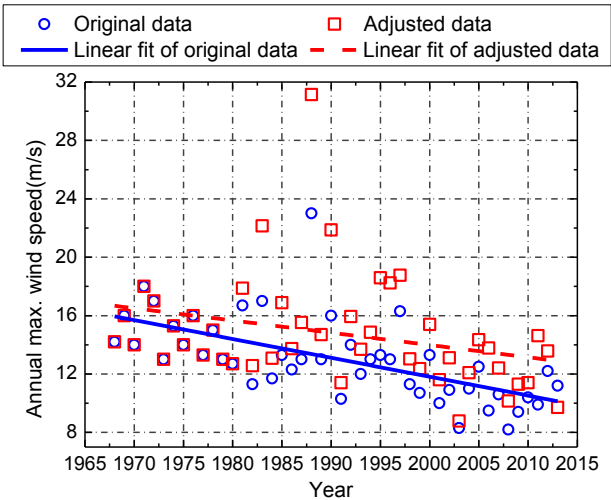


Fig. 9 Comparison between adjusted and original annual maximum wind speed series for Hangzhou station

According to the guide published by world meteorological organization (2012), the exposure correction can only be performed for those data associated with the roughness length no greater than 0.5 m. Therefore, for the exposure correction of wind speed data with larger

roughness length values ($z_0 > 0.5\text{ m}$) along the Direction IV over the period from 2002 to 2010 has been approximately implemented by taking the roughness length value as 0.5 m.

The data series of the adjusted daily maximum wind speed series in the 4 representative wind direction sectors and the adjusted annual maximum wind speed series regardless of wind directions are shown in Figs. 8 and 9, respectively.

2.4 Time-varying trend test for adjusted wind speed series

The regression time-varying trend lines for adjusted daily maximum wind speed series along 4 representative wind direction sectors are depicted in Fig. 8. The Mann-Kendall test results reported in Table 2 confirm the presence of downward trends (as shown in Fig. 8) for the corrected wind speed data along 3 wind direction sectors (i.e., D1, D4 and D10). On the other hand, no monotonic trend was detected for the corrected daily maximum wind speed data in D16 since the probability that supporting the null hypothesis of no monotonic trend is larger than 5%. The regression trend line of the adjusted annual maximum wind speed series was depicted in Fig. 9. The MK test results in Table 3 also support the presence of downward trends of the adjusted annual maximum wind speeds.

The presence of downward trends in the adjusted wind speed series of Hangzhou station may be attributed to non-climate and climate factors. For non-climate factors, although the exposure correction procedure has been conducted on the original wind speed data, it is difficult to completely remove exposure influences. Furthermore, other non-climate factors may still exist. For climate factors, the potential change of winter monsoons may lead to the decreasing trend in the wind speed data series. Xu *et al.* (2006) showed that the surface wind speed associated with the east Asian monsoon has significantly weakened in both winter and summer in the recent three decades. The significant winter warming in northern China may explain the weaken of the winter monsoon while the summer cooling in central south China that may result from air pollution and warming in the western North Pacific Ocean may be responsible for weakening the summer monsoon (Xu *et al.* 2006). Jiang *et al.* (2010) also conducted a research on wind speed changes based on two observational datasets in China from 1956 to 2004, and concluded that the annual mean wind speed, days of strong wind, and maximum wind all show declining trends over broad areas of China. The detected long-term downward trend of the adjusted wind speed series of Hangzhou station in this paper generally agree with previous research work (Xu *et al.* 2006, Jiang *et al.* 2010). It may be necessary to take into account such a non-stationary property of extreme wind speed series in the estimation of design wind speeds with various MRIs for the Hangzhou area. To finish this task, establishing an appropriate nonstationary statistical model is of great importance. For the small-scale nonstationary extreme wind, i.e., thunderstorm or downbursts and tornadoes, many statistical modeling methods including time-varying time series and evolutionary power spectra have been widely used (Chen, 2005, Huang and Chen 2009, Su *et al.* 2015). When it comes to the long-term nonstationary extreme wind speed series, the time-varying

generalized maximum likelihood approach is maybe a good option, which will be addressed in the following section.

3. Non-stationary statistical modeling of extreme wind speed

3.1 Generalized maximum likelihood (GML) approach for parameter estimation

In the classical extreme wind speed analysis, the generalized extreme value (GEV) distribution incorporating Gumbel's type I, Frechet's type II and Weibull's type III distributions is commonly used with constant parameters. Denote the daily/annual maximum wind speed as a random variable V , the cumulative distribution function of which can be modeled by the GEV distribution as:

$$F_V(v) = P(V \leq v) = 1 - p = \exp \left\{ - \left[1 - \frac{\kappa(v - \mu)}{\xi} \right]^{1/\kappa} \right\} \quad \kappa \neq 0$$

$$= \exp \left\{ - \exp \left[- \frac{(v - \mu)}{\xi} \right] \right\} \quad \kappa = 0 \quad (5)$$

in which p denotes the probability of the extreme wind speed V being exceeded by a chosen value of v . μ , $\xi > 0$ and κ are the location, scale and shape parameters, respectively. $\mu + \xi/\kappa \leq v < +\infty$ when $\kappa < 0$ (Frechet); $-\infty < v < +\infty$ when $\kappa = 0$ (Gumbel) and $-\infty < v \leq \mu + \xi/\kappa$ when $\kappa > 0$ (Weibull). Quantiles of the GEV distribution can then be given in terms of the parameters and the exceedance probability p as

$$v_p = \mu + \frac{\xi}{\kappa} \left\{ 1 - \left[-\ln(1-p) \right]^\kappa \right\} \quad \kappa \neq 0$$

$$= \mu - \xi \ln \left[-\ln(1-p) \right] \quad \kappa = 0 \quad (6)$$

For a design wind speed V_R corresponding to a MRI of R days/years, the exceedance probability p of the design wind speed V_R per day/year is equal to $1/R$, then the design wind speed V_R could be estimated by

$$V_R = \mu + \frac{\xi}{\kappa} \left\{ 1 - \left[-\ln \left(1 - \frac{1}{R} \right) \right]^\kappa \right\} \quad \kappa \neq 0$$

$$= \mu - \xi \ln \left[-\ln \left(1 - \frac{1}{R} \right) \right] \quad \kappa = 0 \quad (7)$$

In the non-stationary analysis, the time-varying trend detected in the adjusted extreme wind speed series of Hangzhou station can be taken into account by the GEV model with time-dependent parameters (Coles 2001). Specifically, the location parameter μ_t and the logarithm of the scale parameter $\ln(\xi_t)$ in the non-stationary GEV analysis are assumed to be polynomial functions of covariates $t = 1, 2, \dots, n$ and the shape parameter κ_t is

assumed to be a constant κ , the general form of model parameters can be expressed as

$$\begin{cases} \mu_t = \beta_0 + \beta_1 t + \beta_2 t^2 + \dots \\ \ln(\xi_t) = \delta_0 + \delta_1 t + \delta_2 t^2 + \dots \\ \kappa_t = \kappa \end{cases} \quad (8)$$

where the notations $\beta_0, \beta_1, \beta_2, \delta_0, \delta_1, \delta_2$ are the constant parameters to be estimated. The use of logarithm of the scale parameter instead of itself is aim to ensure the positive value of the scale parameter. The shape parameter is always difficult to estimate with precision, so that it is usually unrealistic to model κ_t as a polynomial function of time.

The next step is to estimate the parameters of the so-called non-stationary GEV model by the maximum likelihood (ML) approach. The vector of parameters is denoted as $\theta = (\beta_0, \beta_1, \beta_2, \dots, \delta_0, \delta_1, \delta_2, \dots, \kappa)$ when $\kappa \neq 0$ and $\theta = (\beta_0, \beta_1, \beta_2, \dots, \delta_0, \delta_1, \delta_2, \dots)$ when $\kappa = 0$. For a set of n extreme wind speed observations (v_1, v_2, \dots, v_n) , the parameters of the non-stationary GEV model can be approximated by maximizing the log-likelihood function (expressed as $\ln[L(\theta|v)]$), the general form of which can be written as

$$\begin{aligned} \ln[L(\theta|v)] &= -n \ln(\xi_t) - \sum_{t=1}^n \left[1 - \kappa \left(\frac{v_t - \mu_t}{\xi_t} \right) \right]^{\frac{1}{\kappa}} - \sum_{t=1}^n \left(1 - \frac{1}{\kappa} \right) \ln \left[1 - \kappa \left(\frac{v_t - \mu_t}{\xi_t} \right) \right] & \kappa \neq 0 \\ &= -n \ln(\xi_t) - \sum_{t=1}^n \frac{v_t - \mu_t}{\xi_t} - \sum_{t=1}^n \exp \left(-\frac{v_t - \mu_t}{\xi_t} \right) & \kappa = 0 \end{aligned} \quad (9)$$

Given the log-likelihood function expressed in Eq. (9), the vector of parameters can be estimated through an equation system formed by setting the partial derivatives of $\ln[L(\theta|v)]$ with respect to each parameter to be zero. Numerical methods such as Newton-Raphson method (Hosking 1985, Macleod 1989) can be utilized to solve the system of equations derived from maximizing Eq. (9). Given the estimated parameters of the non-stationary GEV model, the non-stationary extreme wind speed quantile $V_{R,t}$ with a MRI of R days/years can be estimated by

$$\begin{aligned} V_{R,t} &= \mu_t + \frac{\xi_t}{\kappa} \left\{ 1 - \left[-\ln \left(1 - \frac{1}{R} \right) \right]^{\kappa} \right\} & \kappa \neq 0 \\ &= \mu_t - \xi_t \ln \left[-\ln \left(1 - \frac{1}{R} \right) \right] & \kappa = 0 \end{aligned} \quad (10)$$

It is worth noting that the above ML approach for estimating $V_{R,t}$ can only be used for extreme wind speed observations with large samples, such as daily maximum wind speed series. On the other hand, when applied into small samples like annual maximum wind speed series, absurd value of the shape parameter κ may be generated leading to very high variance of quantile estimation (Hosking *et al.* 1985, Martins and Stedinger 2000). Furthermore, when the shape parameter $\kappa \neq 0$, it is difficult to guarantee that the estimators of the ML approach

meet the desired asymptotic properties (Smith 1985). In order to cope with these limitations, the generalized maximum likelihood (GML) approach is introduced. The GML approach is a Bayesian method based on the same principle as the ML approach with an additional prior information on the shape parameter (Martins and Stedinger 2000, El Adlouni *et al.* 2007). The GML approach assumes that the true shape parameter κ is a random variable with prior distribution $f_{\kappa}(\kappa)$. And the Beta distribution, based on the practical experiences in the area of hydrometeorology (Martins and Stedinger 2000), is applied here as a prior distribution for the shape parameter κ , the probability density function (PDF) of which is expressed as

$$f_{\kappa}(\kappa) = \frac{\Gamma(m+n)(0.5+\kappa)^{m-1}(0.5-\kappa)^{n-1}}{\Gamma(m)\Gamma(n)} = \frac{(0.5+\kappa)^{m-1}(0.5-\kappa)^{n-1}}{B(m,n)} \quad (11)$$

in which the values of m and n were given as $m=6, n=9$ according to Martins and Stedinger (2000). The PDF of Eq. (11) with the interval between $[-0.5, 0.5]$ has mean value of -0.10 and variance of 0.122 for the random shape parameter.

Once the prior distribution of the shape parameter κ is determined, the generalized likelihood function (expressed as $GL(\theta|v)$) can then be written by

$$GL(\theta|v) = L(\theta|v) f_{\kappa}(\kappa) \quad (12)$$

Upon taking logarithm, Eq. (12) becomes

$$\ln[GL(\theta|v)] = \ln[L(\theta|v)] + \ln[f_{\kappa}(\kappa)] \quad (13)$$

Then the vector of parameters $\theta = (\beta_0, \beta_1, \beta_2, \dots, \delta_0, \delta_1, \delta_2, \dots, \kappa)$ can be estimated by maximizing the generalized log-likelihood function $\ln[GL(\theta|v)]$, which is equivalent to maximizing the Bayesian posterior distribution of the parameters, through an equation system formed by setting the partial derivatives of $\ln[GL(\theta|v)]$ with respect to each parameter to zero.

Again the Newton-Raphson method can be used to solve the above equation system. An important advantage of the GML method is the possibility to integrate any additional historical and regional information to refine the prior distributions. When regional information from a number of sites can be utilized to develop a more informative prior distribution for the shape parameter, then substantial improvements in extreme quantile estimations may be achieved.

3.2 Model selection and diagnostics

In the non-stationary analysis, the GEV model with time-dependent parameters may take different forms, i.e., polynomial forms with various degrees in Eq. (8). Before estimating the non-stationary extreme wind speed quantile $V_{R,t}$ with various MRIs, the selection of the proper form to model the time-dependent parameters of the GEV model should be taken into consideration. There are various

polynomial forms of high degree, which might be used for modeling trends in the parameters of the GEV model. A good model is required to adequately describe the underlying climate process that generated the observed wind speed data. Therefore, it is worthwhile to implement model selection and diagnostic for determining the best suitable form of time-dependent parameters in Eq. (8) of the GEV model.

Utilizing the GML method for parameter estimation, the maximum likelihood estimation of candidate models leads to a simple test procedure for model selection. Suppose model M_i is the subset of model M_j , i.e., model M_j has more parameters than model M_i , the deviance statistic for model selection is defined as (Coles 2001)

$$D_{j-i} = 2 \left\{ \max \left\{ \ln [L(M_j)] \right\} - \max \left\{ \ln [L(M_i)] \right\} \right\} \quad (14)$$

where $\max \left\{ \ln [L(M_j)] \right\}$ and $\max \left\{ \ln [L(M_i)] \right\}$ are the maximized log-likelihoods associated with models M_j and M_i respectively. Large value of D_{j-i} suggests that model M_j explains substantially more variation in the data than M_i while small value of D_{j-i} indicates that the increase in model size (i.e., the number of model parameters) of model M_j does not bring significant improvements in the model's capacity to explain the data.

There is a formal criterion can be used to specify how large D_{j-i} should be so that model M_j is preferable to model M_i , which states that model M_i is rejected by a test at a significance level of α if $D_{j-i} > c_{\alpha}^k$, in which c_{α}^k is the $(1-\alpha)$ quantile of the χ_k^2 distribution, and k is the difference in the model size of M_j and M_i .

By use of the deviance statistics, the selection procedure can be hierarchically implemented with the simplest polynomial form of time-dependent parameters (i.e., constant in μ_t and $\ln(\xi_t)$), and if necessary, by adding high degree terms of a polynomial until the deviance statistics show no significant improvement. After selecting the best suitable model among a range of candidate models, there is a need to confirm that the final selected model is actually an adequate representation of the data through model diagnostics. Since the adjusted wind speed data is not assumed to be identically distributed in the non-stationary analysis, it is worthwhile to apply model diagnostic checks to a standardized version of the data conditioned on the estimated parameters, i.e., if the adjusted wind speed data is well represented by a GEV model as

$$V \sim \text{GEV}(\hat{\mu}_t, \hat{\xi}_t, \hat{\kappa}) \quad (15)$$

The standardized wind speed data \tilde{V} can be defined as (Coles 2001)

$$\tilde{V} = -\frac{1}{\hat{\kappa}} \ln \left[1 - \hat{\kappa} \frac{V - \hat{\mu}_t}{\hat{\xi}_t} \right] \quad (16)$$

where each element has the standard Gumbel distribution, with probability distribution function as

$$P(\tilde{V} \leq \tilde{v}) = \exp[-\exp(-\tilde{v})] \quad (17)$$

Denoting the ordered values of the \tilde{v} by $\tilde{v}_{(1)}, \tilde{v}_{(2)}, \dots, \tilde{v}_{(n)}$, the probability plot consists of the data points with: $\left\{ i/(n+1), \exp[-\exp(-\tilde{v}_{(i)})] \right\}; i=1, 2, \dots, n$, while the quantile plot is comprised of the data points with: $\left\{ \tilde{v}_{(i)}, -\ln[-\ln(i/(n+1))] \right\}; i=1, 2, \dots, n$. These two plots can be used to check the fitness of the selected GEV model if a linear trend is observed for the data points.

3.3 Non-stationary model for daily maximum wind speed

The one-year-recurrence extreme wind speed in Hangzhou area can be estimated based on the daily maximum wind speed series in the 16 archived wind direction sectors obtained from the Hangzhou meteorological station.

The downward trends in the adjusted daily maximum wind speed series would be captured by the GEV model with time-dependent parameters, which would be determined by model selection with the aid of the deviance statistics of Eq. (14). Table 5 lists the maximized log-likelihoods of 10 candidate models for the adjusted daily maximum wind speed series in D10. The stationary GEV model for these data (i.e., model M_6) leads to a maximized log-likelihood of -3953.0. A GEV model with a cubic trend in μ and linear trend in $\ln \xi$ (i.e., model M_8) has a maximized log-likelihood of -3922.7. The deviance statistic for comparing these two models is therefore $D_{8-6} = 2 * (-3922.7 + 3953.0) = 60.6$. This value is overwhelmingly large when compared to the $c_{0.05}^4 = 9.49$, which is the (1-5%)

quantile of the χ_4^2 distribution. Comparing M_8 with M_7 , the deviance statistic is $D_{8-7} = 2 * (-3922.7 + 3926.9) = 8.4$. This value is also large on the scale of a χ_1^2 distribution with a (1-5%) quantile of 3.84. Among three models of M_6, M_7 and M_8 , the deviance statistics suggest that the GEV model with a cubic trend in μ and a linear trend in $\ln \xi$ (i.e., model M_8) explains a substantial amount of the temporal trends in the adjusted daily maximum wind speed data, and is able to capture a genuine effect in the variation process rather than a chance feature in the observed data. On the other hand, when considering more complex models with more parameters (i.e., M_9 and M_{10}), there was no evidence supporting the GEV model with either a quartic trend in μ (i.e., model M_9) or a quadratic trend in $\ln \xi$ (i.e., model M_{10}).

The corresponding deviance statistics comparing with the model M_8 are all smaller than the $c_{0.05}^1 = 3.84$, as shown

Table 5 Deviance statistics of various models for adjusted daily maximum wind speed series in D10

Model No.	Model description	Model size (Number of parameters)	Maximized log-likelihood	Deviance statistic result
1	Gumbel-Constant in μ , ξ	2	-4905.8	/
2	Gumbel-Quadratic trend in μ , linear trend in $\ln\xi$	5	-5086.4	/
3	Gumbel-Cubic trend in μ , linear trend in $\ln\xi$	6	-5101.5	$D_{8-3}=2357.6 > c_{0.05}^1 = 3.84$
4	Gumbel-Quartic trend in μ , linear trend in $\ln\xi$	7	-5102.7	/
5	Gumbel-Cubic trend in μ , quadratic trend in $\ln\xi$	7	-5102.0	/
6	GEV-Constant in μ , ξ	3	-3953.0	$D_{8-6}=60.6 > c_{0.05}^4 = 9.49$
7	GEV-Quadratic trend in μ , linear trend in $\ln\xi$	6	-3926.9	$D_{8-7}=8.4 > c_{0.05}^1 = 3.84$
8	GEV-Cubic trend in μ, linear trend in $\ln\xi$	7	-3922.7	/
9	GEV-Quartic trend in μ , linear trend in $\ln\xi$	8	-3921.5	$D_{9-8}=2.4 < c_{0.05}^1 = 3.84$
10	GEV-Cubic trend in μ , quadratic trend in $\ln\xi$	8	-3922.6	$D_{10-8}=0.2 < c_{0.05}^1 = 3.84$

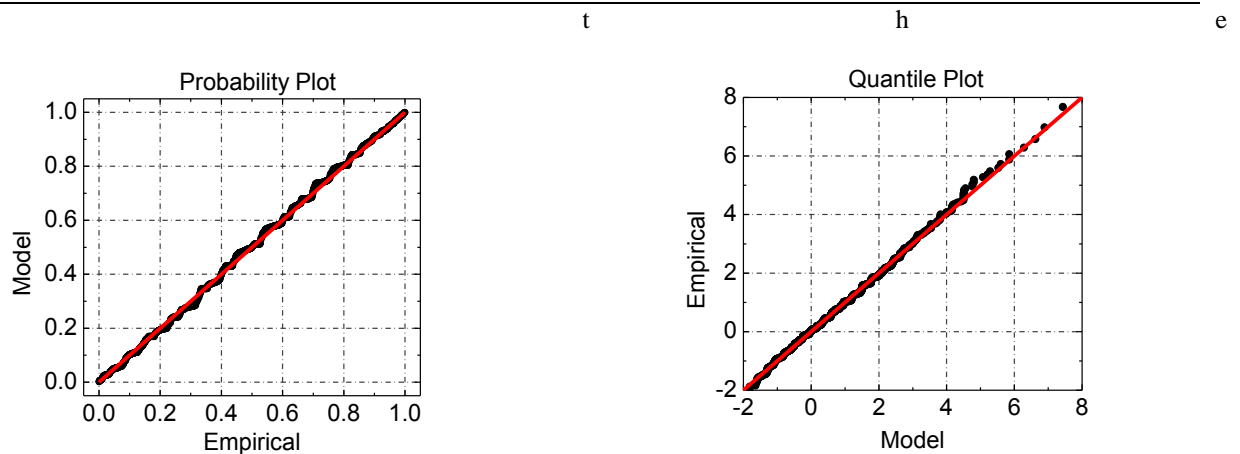


Fig. 10 Diagnostic plots for non-stationary GEV fit to the daily maximum wind speed series in D10

in Table 5. Furthermore, compared to the Gumbel model of M_3 , the associated deviance statistic (i.e., $D_{8-3}=2357.6 > c_{0.05}^1 = 3.84$) implies significant improvement of M_8 over the Gumbel model. Therefore, the GEV model M_8 with a cubic trend in the location parameter and a linear trend in the logarithm of the scale parameter is preferable to other models in Table 5. The quality of the selected GEV model M_8 could be validated by diagnostic plots. As shown in Fig. 10, each set of plotted points is near-linear in both the probability plot and the quantile plot, confirming the accuracy of the selected non-stationary GEV model.

For all the other 15 wind direction sectors, the selected GEV model M_8 with a cubic trend in the location parameter and a linear trend in the logarithm of the scale parameter was also found to be adequate for describing the temporal trends in the adjusted daily maximum wind speed series. Table 6 shows the estimated parameters of the selected GEV model for the adjusted daily maximum wind speed series in 4 representative wind direction sectors (i.e., D1, D4, D10, D16), with 95% confidence intervals in brackets. Based on the estimated parameters of the selected GEV model, the one-year-recurrence extreme wind speed of Hangzhou area for each wind direction sector can be estimated by Eq. (10) with $R=365.25$ days. Fig. 11 shows

corresponding quantiles estimated using the stationary GEV model and the better-fitting non-stationary GEV model in the 4 representative wind direction sectors from the total 16 wind direction sectors as defined in Fig. 3. It can be found that, for a general view, decreasing trends are displayed for the time varying non-stationary quantiles, although these tendencies vary from each wind direction sector. As suggested by the deviance statistics, the selected non-stationary GEV model gives a more faithful representation of the apparent time variation of the adjusted data than the stationary one. Given the time varying non-stationary quantiles for each wind direction sector, the latest one-year-recurrence extreme wind speed can be determined. Fig. 12

displays the point estimations and interval estimations with 95% confidence level for the one-year-recurrence extreme wind speed using the stationary GEV model and the selected non-stationary GEV model at the end of the year of 2013 for 16 wind direction sectors as defined in Fig. 3. By comparing the latest one-year-recurrence extreme wind speed between using the stationary and non-stationary GEV models, it can be observed that the stationary estimates yield larger values than the latest non-stationary ones for all 16 wind direction sectors, implying that it is conservative to implement the conventional stationary

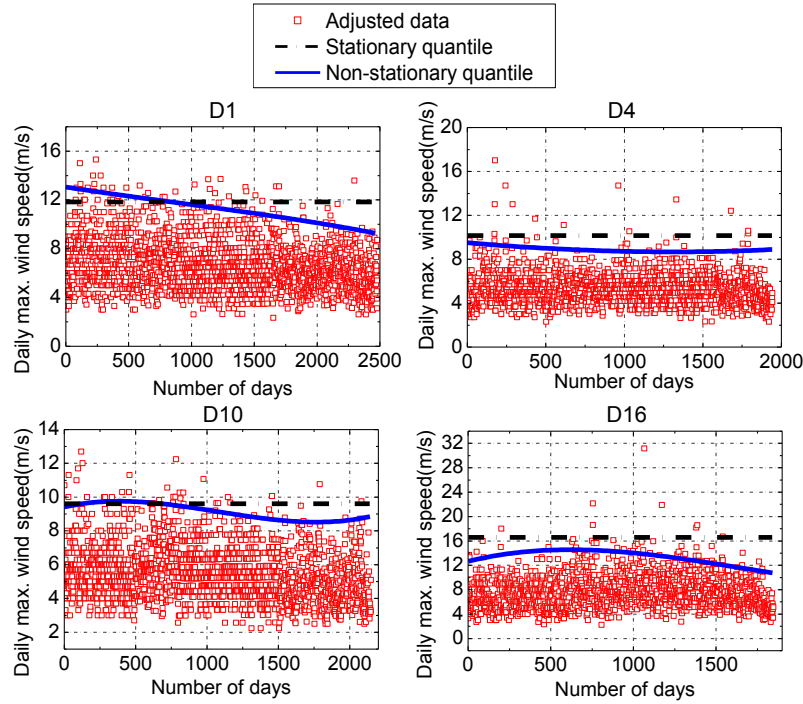


Fig. 11 Estimated one-year-recurrence quantiles using the stationary and non-stationary GEV models

Table 6 Estimated parameters of the non-stationary GEV distribution for adjusted daily max. wind speed

Wind direction	Location parameter (Cubic polynomial)				Scale parameter (linear form)		Shape parameter
	β_0	β_1	β_2	β_3	δ_0	δ_1	κ
1	6.54	-8.30E-04	3.48E-07	-1.05E-10	0.664	-1.70E-04	-0.089
	[6.48,6.59]	[-1E-03,-6.4E-04]	[1.6E-07,5.3E-07]	[-1.6E-10,-5.5E-11]	[0.654,0.674]	[-1.77E-04,-1.63E-04]	[-0.093,-0.085]
4	4.71	3.60E-04	-4.05E-07	1.50E-10	0.079	5.00E-05	-0.104
	[4.64,4.77]	[1.3E-04,5.9E-04]	[-6.2E-07,-1.9E-07]	[9.2E-11,2.1E-10]	[0.067,0.091]	[4.14E-05,5.86E-05]	[-0.109,-0.097]
10	4.86	2.20E-03	-2.89E-06	8.57E-10	0.276	-4.66E-05	-0.094
	[4.78,4.93]	[2.0E-03,2.5E-03]	[-3.1E-06,-2.7E-06]	[8.0E-10,9.2E-10]	[0.264,0.289]	[-5.55E-05,-3.77E-05]	[-0.099,-0.089]
16	5.01	5.55E-03	-4.38E-06	8.28E-10	0.891	-2.67E-04	-0.071
	[4.90,5.12]	[0.005,0.007]	[-4.8E-06,-4.0E-06]	[7.2E-10,9.3E-10]	[0.874,0.908]	[-2.79E-04,-2.54E-04]	[-0.075,-0.066]

statistical modeling to estimate the one-year-recurrence extreme wind speed for the Hangzhou station.

3.4 Non-stationary model for annual maximum wind speed

The time-varying trend of the annual maximum wind speed data as revealed in Fig. 9 could also be captured by the suitable form of GEV model with time-dependent parameters in Eq. (8). Table 7 lists the maximized log-likelihoods of 10 candidate models for the adjusted annual maximum wind speed series in Hangzhou station. From Table 7, the deviance statistics of $D_{2,1}$ and $D_{3,2}$ are 12.76 and 8.26 respectively. Since both values are larger than $c_{0.05}^1 = 3.84$, i.e., the 95% quantile of the χ_1^2 distribution, it follows that the Gumbel model with both linear trends in μ and $\ln \xi$ (i.e., model M_3) is preferable to other two Gumbel models (i.e., model M_1 and M_2) in Table 7. There was also no evidence supporting that the Gumbel models with increasing model size (i.e., model M_4 and M_5) bring

significant improvements over the model of M_3 due to smaller values of the deviance statistic results, i.e., $D_{4,3} = 2.28$ and $D_{5,3} = 1.72$. On the other hand, compared with the corresponding GEV model M_8 , the Gumbel model M_3 is also adequate as the associated deviance statistics $D_{8,3}$ is smaller than $c_{0.05}^1$. Therefore the deviance statistics results listed in Table 7 strongly suggest that the Gumbel model with both linear trends in the location parameter and logarithm of the scale parameter (i.e., model M_3) is the most suitable one for modeling the adjusted annual maximum wind speed series in Hangzhou station. Table 8 reports the estimated parameters of the most suitable non-stationary Gumbel model. Given the sign of the estimated coefficients (i.e., β_i and δ_i in Table 8) of linear terms, it is noted that the location parameter shows a decreasing trend with time variable while the scale parameter presents a slightly increasing trend. The goodness-of-fit of the selected Gumbel model was again confirmed by the standard diagnostic plots, as shown in Fig. 13.

Table 7 Deviance statistics of various models for adjusted annual maximum wind speed series

Model No.	Model description	Model size (Number of parameters)	Maximized log-likelihood	Deviance statistic result
1	Gumbel-Constant in μ , ξ	2	-124.21	$D_{2-1}=12.76>$ $c_{0.05}^1 = 3.84$
2	Gumbel-Linear trend in μ	3	-117.83	$D_{3-2}=8.26>$ $c_{0.05}^1 = 3.84$
3	Gumbel-Linear trend in μ, $\ln\xi$	4	-113.7	/
4	Gumbel-Quadratic trend in μ , linear trend in $\ln\xi$	5	-112.56	$D_{4-3}=2.28<$ $c_{0.05}^1 = 3.84$
5	Gumbel-Linear trend in μ , quadratic trend in $\ln\xi$	5	-112.84	$D_{5-3}=1.72<$ $c_{0.05}^1 = 3.84$
6	GEV-Constant in μ , ξ	3	-127.49	/
7	GEV-Linear trend in μ	4	-119.83	/
8	GEV-Linear trend in μ , $\ln\xi$	5	-115.64	$D_{8-3}=-3.88<$ $c_{0.05}^1 = 3.84$
9	GEV-Quadratic trend in μ , linear trend in $\ln\xi$	6	-113.92	/
10	GEV-Linear trend in μ , quadratic trend in $\ln\xi$	6	-113.87	/

Table 8 Estimated parameters of the non-stationary Gumbel distribution for adjusted annual max. wind speed

Model			Gumbel
Location parameter	β_0	Point estimation	18.624
		Lower 95% Confidence Limit	18.430
		Upper 95% Confidence Limit	18.817
	β_1	Point estimation	-0.063
		Lower 95% Confidence Limit	-0.080
		Upper 95% Confidence Limit	-0.047
Scale parameter	δ_0	Point estimation	1.746
		Lower 95% Confidence Limit	1.736
		Upper 95% Confidence Limit	1.756
	δ_1	Point estimation	0.005
		Lower 95% Confidence Limit	0.004
		Upper 95% Confidence Limit	0.006

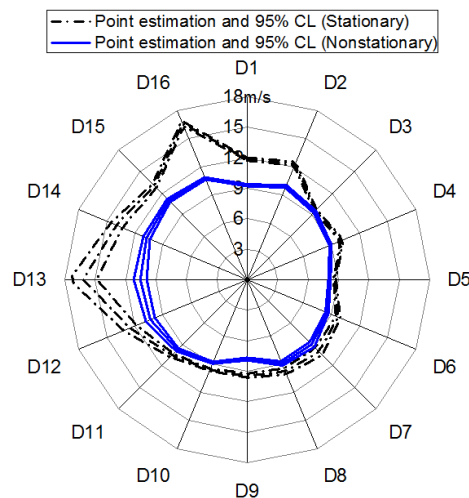


Fig. 12 One-year-recurrence extreme wind speed of Hangzhou station for each wind direction sector

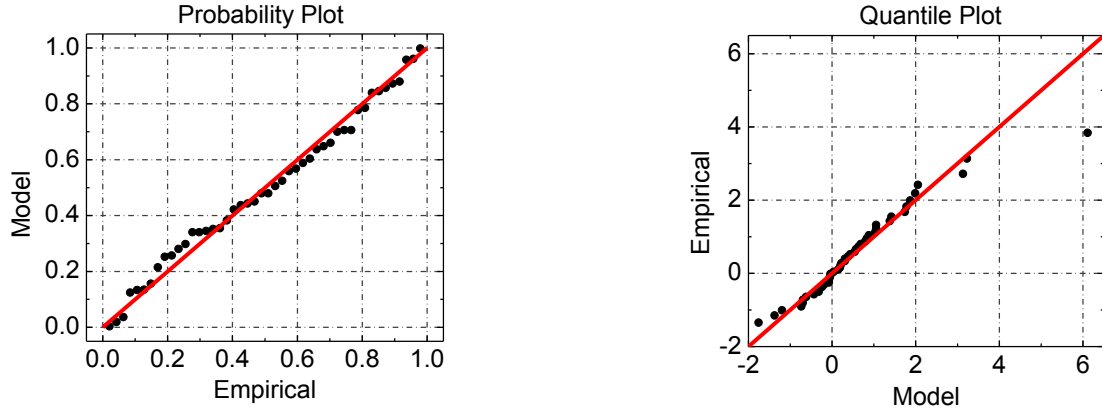


Fig. 13 Diagnostic plots for non-stationary Gumbel fit to the annual maximum wind speed series

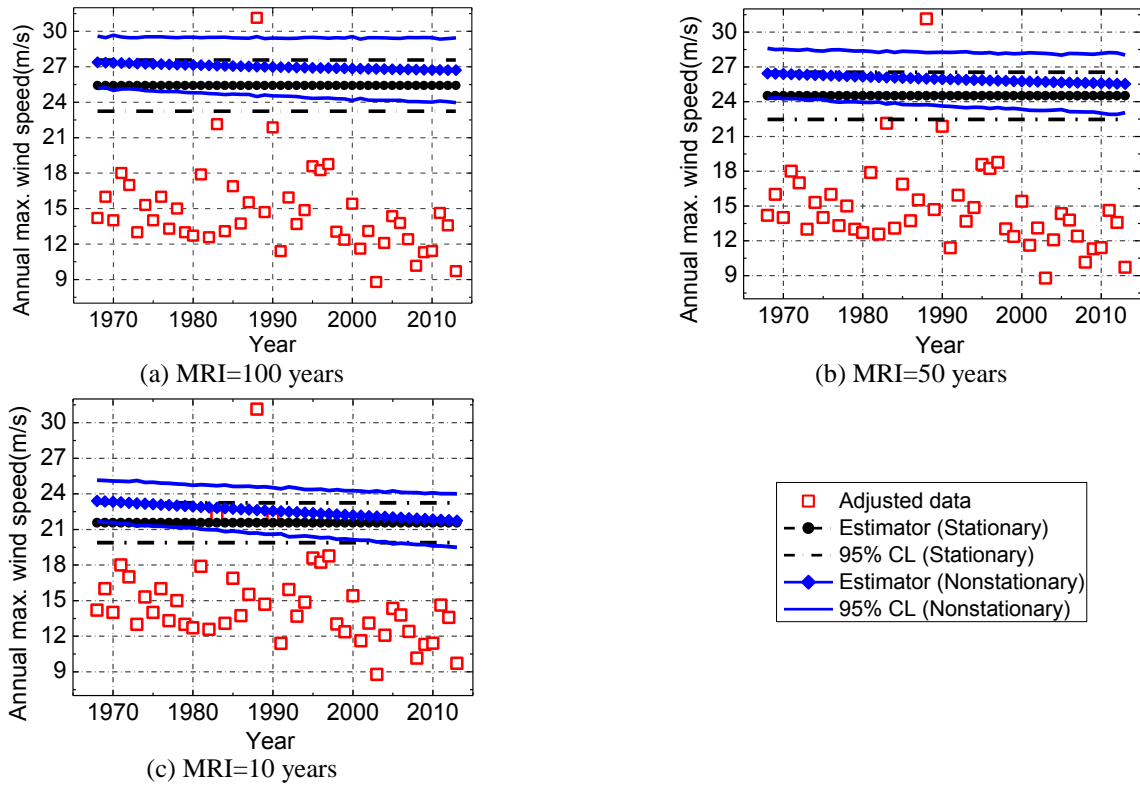


Fig. 14 Estimated quantiles and their confidence limits using the stationary and non-stationary Gumbel models

Once the non-stationary model is determined for the adjusted annual maximum wind speed data, the non-stationary extreme wind speed quantile with various MRIs could be easily estimated from Eq. (10). Fig. 14 shows the estimated “time-dependent” extreme wind speed quantiles and 95% confidence limits by using the non-stationary Gumbel model for various MRIs of 10/50/100 years. The design wind speeds were also estimated by the classical stationary statistical modeling and plotted in Fig. 14. The determined non-stationary Gumbel model is able to take into account the time variation of the adjusted extreme wind speed data series. As a whole, downward trends are displayed for the time varying extreme wind speed quantiles with three different MRIs. Fig. 15 shows the comparison

between estimated quantiles and their 95% confidence limits with various MRIs using the stationary Gumbel model and the selected non-stationary Gumbel model at the end of the year of 2013. As expected, the 95% confidence intervals consistently increase with the increase of MRIs. Such a result indicates that estimation of design wind speed with very large MRIs always involves large uncertainty. By comparing the estimated quantiles between using the stationary and non-stationary Gumbel models, it was found that the non-stationary model yields larger values of design wind speed when the MRI is greater than 8 years. Especially, when the MRI=50/100 years, the design wind speed by using the stationary model is 24.5/25.4 m/s. The corresponding value by using the non-stationary model is

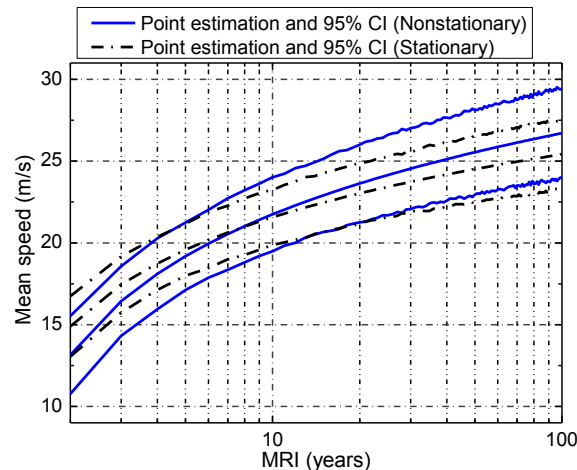


Fig. 15 Comparison between estimated quantiles and their confidence limits with various MRIs using the stationary and non-stationary Gumbel models

25.5/26.7 m/s respectively, which is 4%/5% larger than those estimated by the stationary model. That is to say the conventional stationary statistical modeling may underestimate the design wind speeds associated with common used 10, 50 and 100 MRIs.

4. Conclusions

Based on the surface wind observations of the Hangzhou meteorological station in China, obvious long-term downward trends were detected in the original daily/annual maximum wind speed series by utilizing the Mann-Kendall test. This presence of temporal trends in the extreme wind speed series of Hangzhou station may be partially attributed to the non-climate factors such as time varying exposure, problems with standardization of the wind speed data and so on. An exposure correction procedure was adopted in this paper attempting to correct the original extreme wind speed series to the standard exposure category.

In order to take into account the time-varying trends of extreme wind speed series in Hangzhou area, non-stationary statistical modeling of the adjusted daily/annual maximum wind speed data were implemented using the GEV model with time-dependent parameters. For the adjusted daily maximum wind speed data of the Hangzhou station, the GEV model with a cubic trend in the location parameter and a linear trend in the logarithm of the scale parameter was identified as the most preferable model through model selection and diagnostics. The Gumbel model with both linear trends in the location parameter and logarithm of the scale parameter was found to be the best suitable one for modeling the adjusted annual maximum wind speed data in Hangzhou station. Based on the determined non-stationary models of extreme wind speed, the one-year-recurrence extreme wind speed and extreme wind speed quantiles (i.e., time-dependent “design wind speeds”) with various MRIs were estimated. The estimated time-dependent design wind speed results show that the conventional stationary extreme

value modeling may underestimate design wind speed estimations in Hangzhou area associated with common used 10, 50 and 100 MRIs. Although his finding is mainly concerned about Hangzhou area, the similar non-stationary statistical modeling process can be used for extreme wind speed estimation in other area. Since the temporal trends of surface wind speed observations were detected from many meteorological stations in China, it is necessary to carefully consider the non-stationary property of extreme wind speed observations for particular regions. It should be noted that the daily maximum wind speed data used in the analysis might be related to various long-term wind climatology (synoptic winds, typhoons) or short-term transient extreme wind events (downbursts, thunderstorms and cyclones).

Acknowledgements

The work described in this paper was partially supported by the National Natural Science Foundation of China (Project No.51578504, No.51508502).

References

- Aboshosha, H., Bitsuamlak, G. and Damatty, A.E. (2015), “Turbulence characterization of downbursts using LES”, *J. Wind Eng. Ind. Aerod.*, **136**(136), 44-61.
- Aboshosha, H. and Damatty, A.E. (2015), “Engineering method for estimating the reactions of transmission line conductors under downburst winds”, *Eng. Struct.*, **99**, 272-284.
- AJ-RLB (2004), Recommendations for loads on buildings. Architectural Institute of Japan, Tokyo.
- Ashcroft, J. (1994), “The relationship between the gust ratio, terrain roughness, gust duration and the hourly mean wind speed”, *J. Wind Eng. Ind. Aerod.*, **53**(3), 331-355.
- BS EN 1991-1-4 (2005), Eurocode 1: Actions on Structures - Part 1-4: General actions - Wind Actions, European Committee for Standardization, British Standards Institution, London.
- Chen, K., Jin, X.Y. and Qian, J.H. (2012), “Calculation method on the reference wind pressure accounting for the terrain variations”, *Acta Sci. Nat. Univ. Pekin.*, **48**(1), 13-19 (in

- Chinese).
- Coles, G.S. (2001), *An Introduction to Statistical Modeling of Extreme Values*, Springer, New York.
- Cook, N.J. (1985), *The Designer's Guide to Wind Loading on Building Structures. Part I: Background, Damage Survey, Wind Data, and Structural Classification*. Building Research Establishment, Watford.
- Cook, N.J. and Harris, R.I. (2004), "Exact and general FT1 penultimate distributions of extreme wind speeds drawn from tail-equivalent Weibull parents", *Struct. Saf.*, **26**(4), 391-420.
- Chen, L. (2005), *Vector time-varying autoregressive (TVAR) models and their application to downburst wind speeds*, Ph.D. Dissertation, Texas Tech University.
- Dyrbye, C. and Hansen, S.O. (1996), *Wind Loads on Structures*. John Wiley & Sons, New York.
- El Adlouni, S., Ouarda, T.B.M.J., Zhang, X., Roy, R. and Bobée, B. (2007), "Generalized maximum likelihood estimators for the non-stationary generalized extreme value model", *Water Resour. Res.*, **43**(3).
- GB 50009-2012. *Load Code for the Design of Building Structures*, Ministry of Housing and Urban-Rural Development of the People's Republic of China. China Architecture & Building Press (in Chinese).
- Gilbert, R.O. (1987), *Statistical Methods for Environmental Pollution Monitoring*, Wiley, NY.
- Harris, R.I. (2009), "XIMIS, a penultimate extreme value method suitable for all types of wind climate", *J. Wind Eng. Ind. Aerod.*, **97**(5-6), 271-286.
- Harris, R.I. and Cook, R.J. (2014), "The parent wind speed distribution: Why Weibull?", *J. Wind Eng. Ind. Aerod.*, **131**, 72-87.
- Holmes, J.D. and Moriarty, W.W. (1999), "Application of the generalized Pareto distribution to extreme value analysis in wind engineering", *J. Wind Eng. Ind. Aerod.*, **83**(1), 1-10.
- Hosking, J.R.M. (1985), "Algorithm AS 215: Maximum-likelihood estimation of the parameters of the generalized extreme-value distribution", *J. Roy. Stat. Soc. Series C (Applied Statistics)*, **34**(3), 301-310.
- Hosking, J.R.M., Wallis, J.R. and Wood, E.F. (1985), "Estimation of the generalized extreme-value distribution by the method of probability-weighted moments", *Technometrics*, **27**(3), 251-261.
- Hundechea, Y., St-Hilaire, A., Ouarda, T.B.M.J., El Adlouni, S. and Gachon, P. (2008), "A nonstationary extreme value analysis for the assessment of changes in extreme annual wind speed over the Gulf of St. Lawrence", *Can. J. Appl. Meteorol. Clim.*, **47**(11), 2745-2759.
- Huang, G. and Chen, X. (2009), "Wavelets-based estimation of multivariate evolutionary spectra and its application to nonstationary downburst winds", *Eng. Struct.*, **31**(4), 976-989.
- Huang, G., Zheng, H., Xu, Y.L. and Li, Y. (2015), "Spectrum models for nonstationary extreme winds", *J. Struct. Eng.*, **141**(10), 04015010.
- Jiang, Y., Luo, Y., Zhao, Z. and Tao, S. (2010), "Changes in wind speed over China during 1956-2004", *Theor. Appl. Climatol.*, **99**(3-4), 421-430.
- Kasperski, M. (2009), "Specification of the design wind load-A critical review of code concepts", *J. Wind Eng. Ind. Aerod.*, **97**(7-8), 335-357.
- Katz, R.W., Parlange, M.B. and Naveau, P. (2002), "Statistics of extremes in hydrology", *Adv. Water Resour.*, **25**(8), 1287-1304.
- Kendall, M.G. (1975), *Rank Correlation Methods*, 4th Ed., Charles Griffin, London.
- Kharin, V.V. and Zwiers, F.W. (2005), "Estimating extremes in transient climate change simulations", *J. Climate*, **18**(8), 1156-1173.
- Li, Z.X., He, Y., Wang, P., Theakstone, W. H., An, W., Wang, X. and, Cao, W. (2012), "Changes of daily climate extremes in southwestern China during 1961-2008", *Global and Planetary Change*, **80**, 255-272.
- Lombardo, F.T., Main, J.A. and Simiu, E. (2009), "Automated extraction and classification of thunderstorm and non-thunderstorm wind data for extreme-value analysis", *J. Wind Eng. Ind. Aerod.*, **97**(3), 120-131.
- Lombardo, F.T. (2012), Improved extreme wind speed estimation for wind engineering applications. *J. Wind Eng. Ind. Aerod.*, **104-106**, 278-284.
- Lombardo, F.T. (2014), "Extreme wind speeds from multiple wind hazards excluding tropical cyclones", *Wind Struct.*, **19**(5), 467-480.
- Lombardo, F.T. and Ayyub, B.M. (2015), "Analysis of Washington, DC, wind and temperature extremes with examination of climate change for engineering applications. ASCE-ASME", *J. Risk Uncertainty in Eng. Syst., Part A: Civil Eng.*, **1**(1), 04014005.
- Lombardo, F.T. and Krupar III, R.J. (2016), "A comparison of aerodynamic roughness length estimation methods for use in characterizing surface terrain conditions", submitted to *J. Struct. Eng.*
- Macleod, A.J. (1989), "A remark on algorithm AS 215: Maximum-likelihood estimation of the parameters of the generalized extreme-value distribution", *Appl. Statist.*, **38**(1), 198-199.
- Mann, H.B. (1945), "Non-parametric tests against trend", *Econometrica*, **13**, 163-171.
- Martins, E.S. and Stedinger, J.R. (2000), "Generalized maximum-likelihood generalized extreme-value quantile estimators for hydrologic data", *Water Resour. Res.*, **36**(3), 737-744.
- Masters, F.J., Tieleman, H.W. and Balderrama, J.A. (2010a), "Surface wind measurements in three gulf coast hurricanes of 2005", *J. Wind Eng. Ind. Aerod.*, **98**(10-11), 533-547.
- Masters, F.J., Vickery, P.J., Bacon, P. and Rappaport, E.N. (2010b), "Toward objective, standardized intensity estimates from surface wind speed observations", *Bull. Am. Meteorol. Soc.*, **91**(12), 1665-1681.
- Miller, C., Balderrama, J.A. and Masters, F. (2015), "Aspects of observed gust factors in landfalling tropical cyclones: gust components, terrain, and upstream fetch effects", *Bound.- Lay. Meteorol.*, **155**(1), 1-27.
- Mo, H.M., Hong, H.P. and Fan, F. (2015), "Estimating the extreme wind speed for regions in China using surface wind observations and reanalysis data", *J. Wind Eng. Ind. Aerod.*, **143**, 19-33.
- Pagnini, L.C. and Solari, G. (2015), "Joint modeling of the parent population and extreme value distributions of the mean wind velocity", *J. Struct. Eng.*, **142**(2), 04015138.
- Palutikof, J.P., Brabson, B.B., Lister, D.H. and Adcock, S.T. (1999), "A review of methods to calculate extreme wind speeds", *Meteorol. Appl.*, **6**(2), 119-132.
- Pavia, E.G. and O'Brien, J.J. (1986), "Weibull statistics of wind speed over the ocean", *J. Clim. Appl. Meteorol.*, **25**(10), 1324-1332.
- Ruest, B., Neumeier, U., Dumont, D., Bismuth, E., Senneville, S. and Caveen, J. (2016), "Recent wave climate and expected future changes in the seasonally ice-infested waters of the Gulf of St. Lawrence", *Can. Clim. Dynam.*, **46**(1-2), 449-466.
- Sacré, C., Moisselin, J.M., Sabre, M., Flori, J.P. and Dubuisson, B. (2007), "A new statistical approach to extreme wind speeds in France", *J. Wind Eng. Ind. Aerod.*, **95**(9-11), 1415-1423.
- Simiu, E. and Heckert, N.A. (1996), "Extreme wind distribution tails: a 'peaks over threshold' approach", *J. Struct. Eng.*, **122**(5), 539-547.
- Smith, R.L. (1985), "Maximum likelihood estimation in a class of non-regular cases", *Biometrika*, **72**(1), 67-90.
- Solari, G., Repetto, M. P., Burlando, M., De Gaetano, P., Pizzo, M., Tizzi, M. and Parodi, M. (2012), "The wind forecast for safety

- management of port areas”, *J. Wind Eng. Ind. Aerod.*, **104**, 266-277.
- Su, Y., Huang, G. and Xu Y. (2015), “Derivation of time-varying mean for non-stationary downburst winds”, *J. Wind Eng. Ind. Aerod.*, **141**, 39-48.
- Tuller, S.E. and Brett, A.C. (1984), “The characteristics of wind velocity that favor the fitting of a Weibull distribution in wind speed analysis”, *J. Clim. Appl. Meteorol.*, **23**(1), 124-134.
- World meteorological organization (2012), Guide to Meteorological Instruments and Methods of Observation. Secretariat of the World Meteorological Organization.
- Xu, M., Chang, C.P., Fu, C., Qi, Y., Robock, A., Robinson, D. and Zhang, H.M. (2006), “Steady decline of east Asian monsoon winds, 1969-2000: Evidence from direct ground measurements of wind speed”, *J. Geophys. Res: Atmos.*, **111**(D24).
- Xu, Y.L., Hu, L. and Kareem, A. (2014), “Conditional simulation of nonstationary fluctuating wind speeds for long-span bridges”, *J. Eng. Mech.*, **140**(1), 61-73.
- Yan, Z., Bate, S., Chandler, R.E., Isham, V. and Wheeler, H. (2006), “Changes in extreme wind speeds in NW Europe simulated by generalized linear models”, *Theor. Appl. Climatol.*, **83**(1-4), 121-137.
- Yang, X., Li, Z., Feng, Q., He, Y., An, W., Zhang, W. *et al.* (2012), “The decreasing wind speed in southwestern china during 1969–2009, and possible causes”, *Quaternary Int.*, **263**(3), 71-84.
- Ying, M., Zhang, W., Yu, H., Lu, X., Feng, J., Fan, Y. *et al.* (2014), “An overview of the China Meteorological Administration tropical cyclone database”, *J. Atmos. Oceanic Technol.*, **31**(2), 287-301.
- You, Q., Kang, S., Aguilar, E., Pepin, N., Flügel, W. A., Yan, Y. and Huang, J. (2011), “Changes in daily climate extremes in China and their connection to the large scale atmospheric circulation during 1961–2003”, *Clim. Dynam.*, **36**(11-12), 2399-2417.
- Zhang, X., Zwiers, F.W. and Li, G. (2004), “Monte Carlo experiments on the detection of trends in extreme values”, *J. Climate*, **17**(10), 1945-1952.
- Zwiers, F.W. and Kharin, V.V. (1998), “Changes in the extremes of the climate simulated by CCC GCM2 under CO2 doubling”, *J. Climate*, **11**(9), 2200-2222.